Turkish Online Journal of Qualitative Inquiry (TOJQI)
Volume 12, Issue 8, July 2021: 2090-2102

Design of CNTFET based Biosensor Interface Circuit for Array Sensors

Radha B. L.[1], Cyril Prasanna Raj P[2], Dinesh Rangappa[3]

[1]Research Scholar, VTU RRC, Belgavi, Associate Professor, Dept. of ECE, BIT,radhablrbl@gmail.com

[2]Dr.,Professor, Dept. Of ECE, Cambridge Institute of Technology, IEEE Senior Member,cyrilyahoo@gmail.com
[3]Dr., Professor, Dept. Of Nanotechnology, VTU CPGS VIAT Muddenahalli,dineshrangappa @gmail.com

Abstract

FET based biosensors are more promising devices for detecting cancer due to cost benefits, faster response and simple approach. For a biosensor to be used in a real environment for both clinical and lab applications, the electronic circuits that process the signals from biosensors and identify the changes in signal properties is a significant activity. The design of interface circuits and signal conditioning circuits need to be designed according to the biosensor responses.In this work, the design of a biosensor array interfacing circuit is carried out using CNTFETs. In order to improve the sensor performances, sensor arrays are developed. The design of sub-circuits for interfacing circuits and signal conditioning circuits is also presented. The sensitivity is enhanced with a sensor array model that has eight columns of series-connected biosensors. The 8x8 array model is interfaced with an instrumentation amplifier. The analog readout circuit is designed with a reference electrode for the real-time comparison of the sensor array model. All of the circuits are designed using CNTFETs, modelled using SPICE coding and simulated in SPICE environment.

Keywords: *CNTFET, SPICE coding, Biosensor, biosensor array interface circuit*

Introduction

Carbon Nano Tubes (CNT) is a lightweight hexagonal structure made up of graphene sheets or tubes. The electronic conduction property of CNT is an advantage in addition to electrostatic control of the channel. CNTFET based sensors are reported to be highly sensitive, selective, operates at low temperatures providing faster response time and recovery time. These sensors also offer label free detection and stability. The CNT used as a channel connecting the source and drain of the FET can be modified by the chemical destruction of side walls or C-C bonds to generate new surfaces of a carboxyl group and hydroxyl group. The modified surfaces can be attached with functional groups to attract target molecules. The functional molecules attached to the surfaces are fluorescent labelled molecules, antigens, DNA, etc. Ni et al. have introduced –COOH derivative on CNT surface through oxidation reaction and introduced aminopyridine and aminoethyl mercaptan catalyst phthalocyanine (VE-H). Dendrimer with poly attached with divalent platinum metal catalyst on the surface of CNT using –COOH derivative group is carried out by Rezaie et al. Another method of making the CNTFET work as a biosensor is to perform non-covalent modification of the surface through the hybridization of atoms. The non-covalent modification includes dispersion force, hydrogen bonds, π-π stacking and dipole bonds. Metal iridium complex catalyst is coated on CNT using non-covalent

bond by Liu et al. Dalton et al. have used conjugated poly-phenylene vinylene for non-covalent bonding to study dispersion in the polymer matrix. Sodium lauryl sulphate is used for non-covalent bonding using ultrasound. It is observed that by coating CNT with sodium benzoate and sodium dodecylbenzene sulfonate has increased the solubility in water.

The work carried out by Villamizar reports developing salmonella antibodies that functionalize CNTFET to detect salmonella detection with concentrations of 100 colony-forming units (CFU/mL). Similar work is also carried out by So et al. in detecting Escherichia coli. It is observed that the conductivity of the device is reduced by 50% in the presence of Escherichia coli. The current in the CNTFET device is reduced from 3 μA to 1 μA with concentrations of Salmonella varying between 100 CFU/mL to 300 CFU/mL. CNTFET used in detecting Prostate Specific Antigen and the current measurements of PSA detection has been reported by Kim et al. With the increase in PSA-ACT concentration from 0 ng/ml to 100 ng/mL; the electrical signal is found to increase from 1 G/Gs to 1.2 G/Gs. Dastagir et al. in their work have reported the design of FET based sensor for detecting hepatitis C virus (HCV), and it is observed that with a change in concentration of RNA from 0.2 to 0.5 pM, the current is found to change from 50 nA to 200 nA indicating the presence of HCV concentration in the analyte. Similar work carried out for detection of H5N1 is reported by Thu et al. The CNT is used as a conductor channel that changes its signal strength when the H5N1 virus binds with the receptors on the CNT surface. The sensitivity of the device is 0.28 nM/nA for detection concentration limited to 1.25 pM. The drain current is found to vary by 10-2 with gate voltage change of 8 V. The CNT biosensors have been extensively used for biological parameter sensing, and the output of CNTFET is in terms of drain current changes that are observed in response to change in concentration. The drain current is in the nA and μA for any change in the biological parameter concentration, and the variations in drain current are very low, and this requires an accurate interfacing circuit to detect these changes. In order to improve the sensing capability, array sensors are being used.

Operational amplifier design

Figure 1 presents the circuit schematic of CNTFET based two stage operational amplifier circuit. Table 1 presents the OPAMP design specifications considered for the requirement of signal conditioning circuits. The slew rate is assumed to be greater than 1V/ μS, and the power dissipation is set to be less than 10 μW with mobility factors considered from model file the constants K'_p and K'_n are computed.

Table 1*OPAMP design specifications*

Parameters	**Value**
Slew Rate = SR	>1V/μS
V_{out} range	= ±1.5V
ICMR	= 0.15 to 1.2V
Power Dissipation	≤ 10μW
$V_{th} = \|V_{tp}\|$	= 0.25V to 0.45V
$K'_p = \mu_p C_{ox}/2$	= -455 μA/V²
$K'_n = \mu_n C_{ox}/2$	= 1085 μA/V²

The design procedure for MOSFET based OPAMP is discussed in detail by Allen Hollberg. In this work, the design procedure is fine tuned to compute the transistor geometries of CNTFETs for OPAMP circuit schematic.

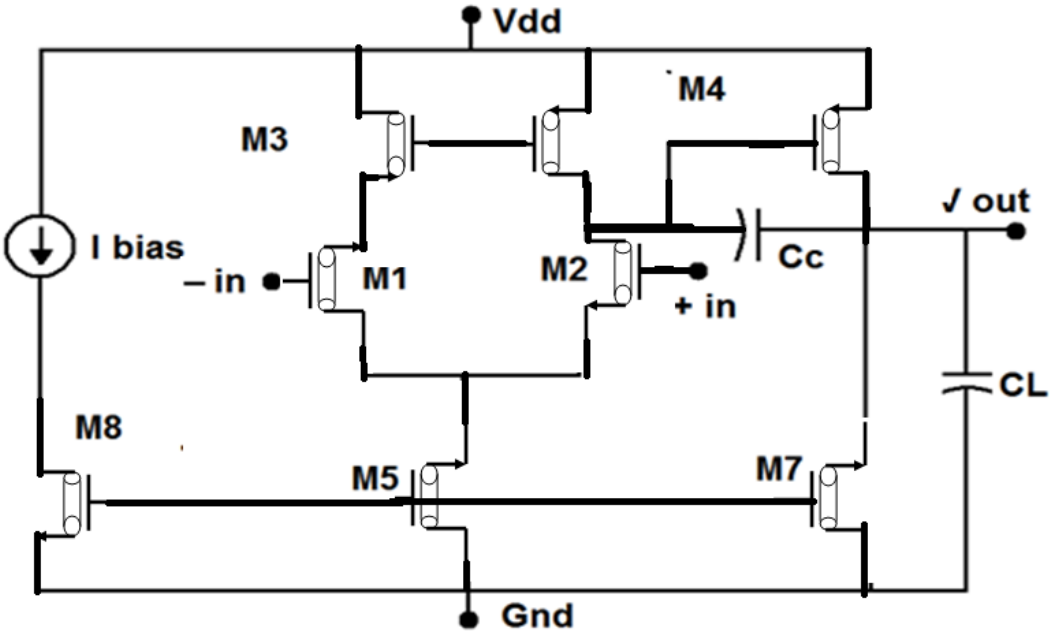

Figure 1. Two stage CNTFET based operational amplifier

The schematic is captured in SPICE environment and simulated in HSPICE for DC and AC response. Output voltage swing, CMRR, PSSR and settling time is also analyzed. The frequency response of the designed OPAMP is also captured for different input voltages from which the gain margin and phase margin is computed. Figure 2 presents the gain margin and phase margin response for OPAMP. The design specifications were set to 60° of PM; from the simulation results, the PM is obtained to be 58°. The UGB measured from the response plot is found to be approximately 1 GHz demonstrating the wider operating range of the designed OPAMP.

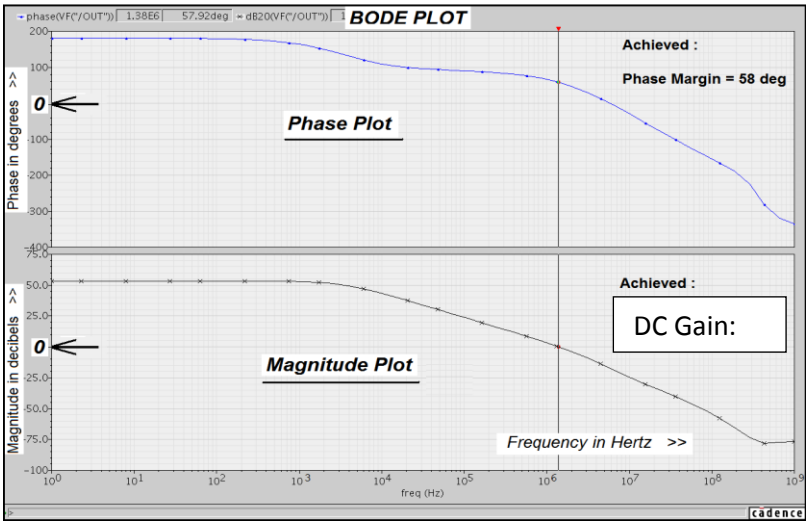

Figure 2. Frequency response representing gain and phase margin

Figure 3 presents the comparator design of OPAMP circuit with DC voltage set to 0V. The comparator output switches between +/- Voltage rails demonstrating functionality.

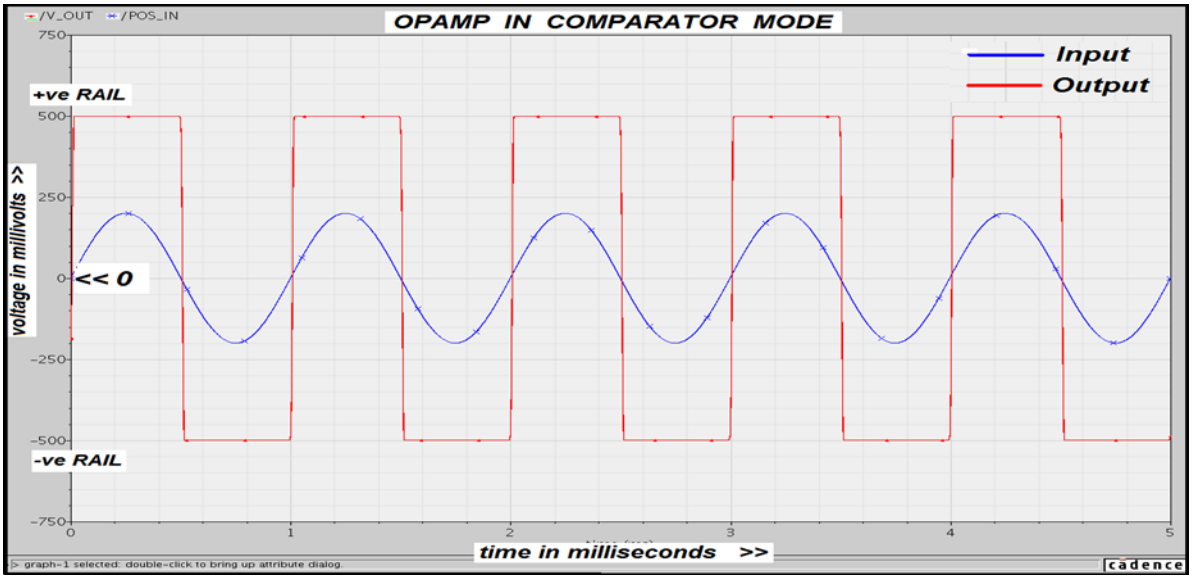

Figure 3. OPAMP configured as comparator

The results obtained in this work for the opamp design is verified and evaluated. The comparisons in terms of PSRR, UGB, SLEW RATE and power dissipation is presented in Table 2. The parameters are considered for the operating frequency of 1 GHz.

Table 2 *Comparison of OPAMP metrics*

Parameters in OPAMP Design	**Existing Literature using 32nm CNTFET technology**	**Present work using 22nm CNTFET technology**
DC Gain	42 dB	53 dB
PSRR	32.4dB	45dB
SLEW RATE	26.36V/µS	10V/µS
Power Dissipation	58µW	12µW
FOM	5.3	52.5

Comparing the performances in terms of PSRR, slew rate, power dissipation and Figure of Merit (FOM), the proposed FINFET based opamp is superior in its performances. The systematic design approach has enabled to design the transistor geometries and the selection of suitable device parameters.

Biosensor interface circuit

The interface circuit for sensing the changes in biosensor current or voltage is designed using a CNTFET device. The operational amplifier that forms the subsystem of the interface circuit is considered and is integrated with passive components to design the interface circuit. Figure 4 presents the interface circuit for the biosensor device.

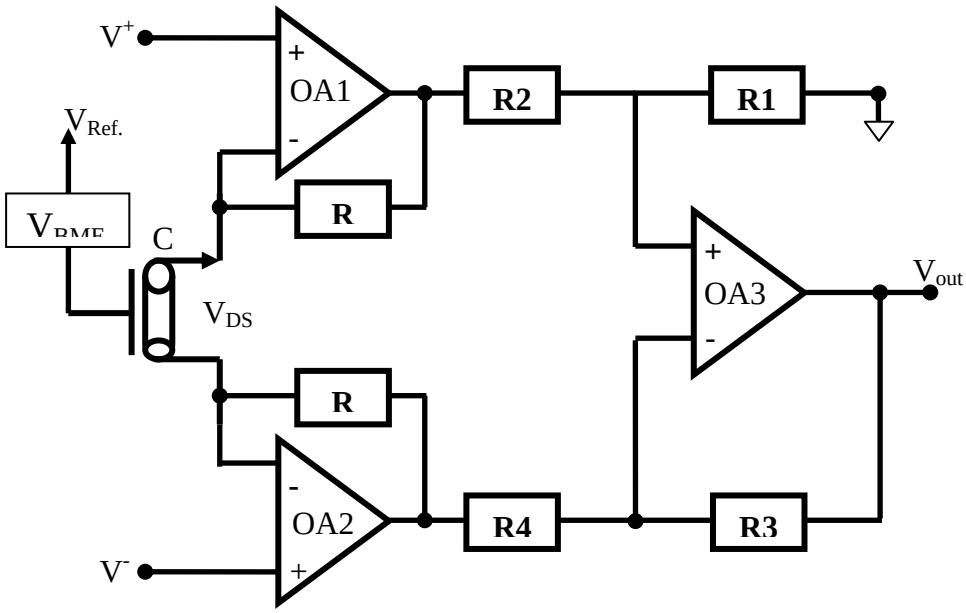

Figure 4. Instrumentation amplifier for biosensor

The difference in voltage that occurs across Vds is measured by the instrumentation amplifier. The feedback resistor is isolated from the input to achieve closed loop gain. The input from the biosensor device is amplified with two voltage followers, and the difference of this voltage is further amplified in the second stage of the amplifier. CMRR and input impedance of instrumentation amplifier are very high, offering good sensitivity to changes in Vds.

$$V_{OUT} = (V_2 - V_1)\left[1 + \frac{2R_2}{R_1}\right]\left(\frac{R_4}{R_3}\right) \quad (1)$$

The voltage Vout at the output of the instrumentation amplifier is given as in Eq. (1). The difference in V1 and V2 are captured and amplified with gain at the output. In order to evaluate the instrumentation amplifier in Figure 4, the SPICE model is developed and the Vref. voltage is set to 0.1 V, and VBMEP voltage is set between 0.01 V to 0.05 V, which is equivalent to electro potential for different pH levels. Figure 5 presents the Vg (Vg = Vref. + V_{BMEP}) and Vout relations in the instrumentation amplifier. With the increase in pH concentration, the sensitivity of the instrumentation amplifier is also increased. The maximum voltage that is available at the output of the instrumentation amplifier is 0.2 V.

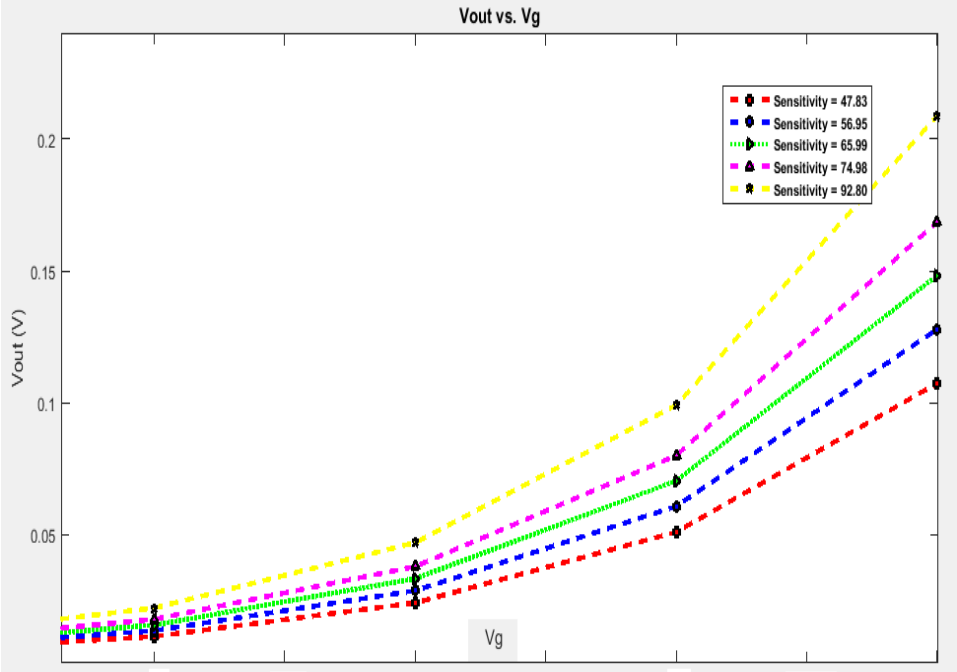

Figure 5. Sensitivity of instrumentation amplifier

In order to increase the sensitivity of detection, the sensor array model is designed, as shown in Figure 6. In the biosensor array model, 64 CNTFET biosensors are considered and arranged in 8 x 8 arrays. The first column of devices is connected in series, and the voltages across the drain and source of the first CNTFET device and last (A^{+}_{1} and $A^{-}_{1,}$ respectively) CNTFET device are connected to the instrumentation amplifier. Similarly, the voltages across all the series connected columns of devices are considered as inputs to the instrumentation amplifier. Each of the CNTFET devices labelled as (Cn) is connected to a reference gate voltage Vref.

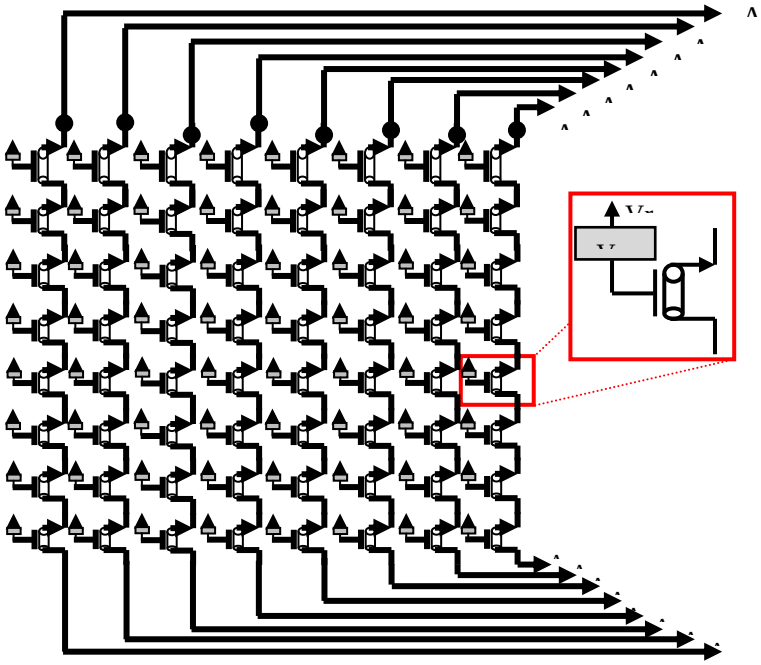

Figure 6. Biosensor array model

The gate voltage (Vg) of each of the CNTFET devices is given as Vg = Vref. + VBMEP. VBMEP is the electro potential voltage due to the biomarker-bioreceptor reaction. As eight devices are connected in series, the total voltage is the sum of all the eight voltages across the biosensor device that is amplified by the instrumentation amplifier for detecting the changes in the biosensor. Figure 7 presents the interface circuit for the first column of the biosensor model shown in Figure 6.

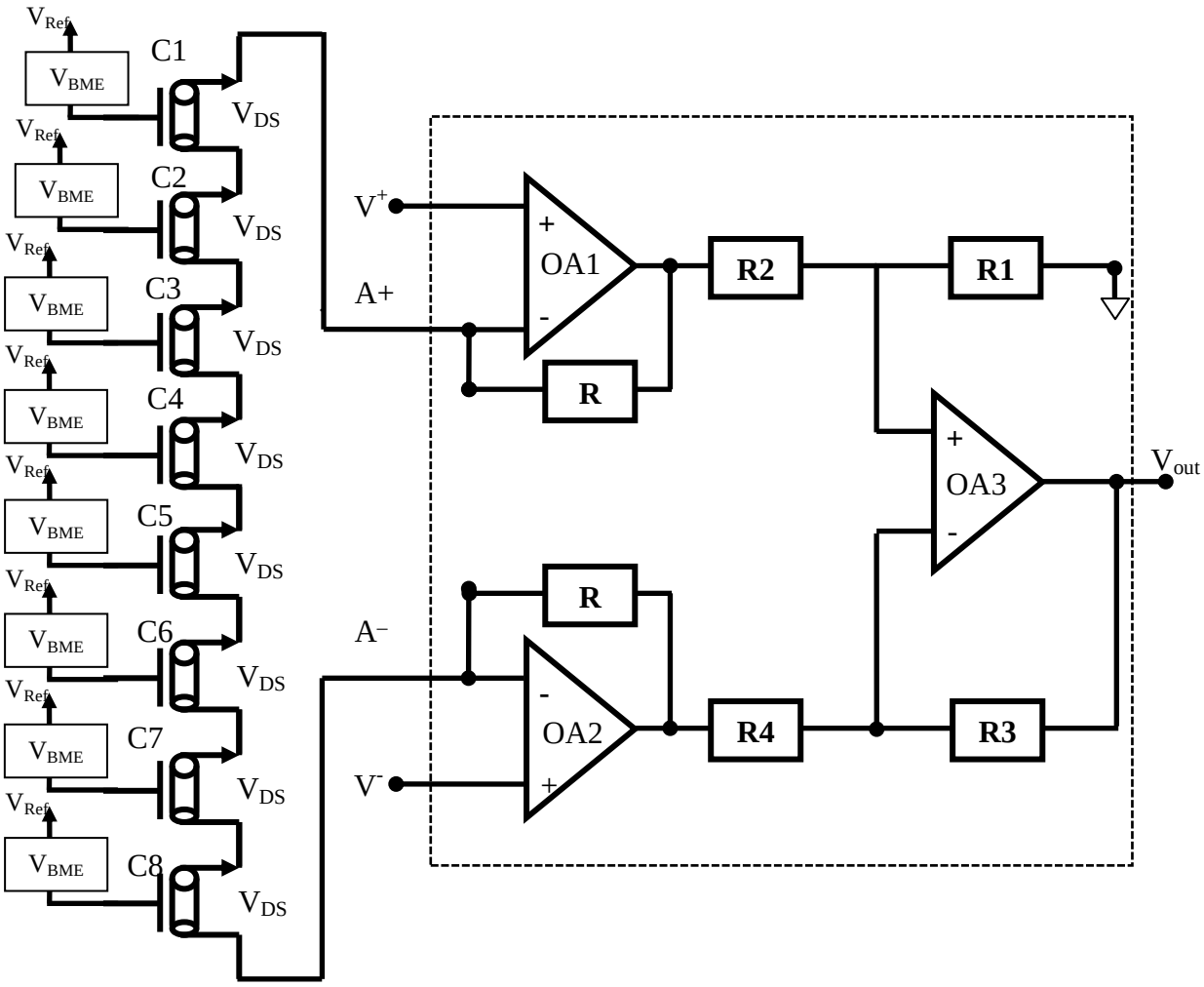

Figure 7. Interface circuit for biosensor array model

As the biosensors are connected in series, the total voltage across the drain-source terminal will be 8Vds which will be sensed by the difference amplifier and amplified by the second stage of the instrumentation amplifier. The biosensor array model has eight columns that generate eight outputs of A^{+}_{n} and A^{-}_{n} (n = 1 to 8), and all eight outputs are processed to generate the final output of the sensor array model.

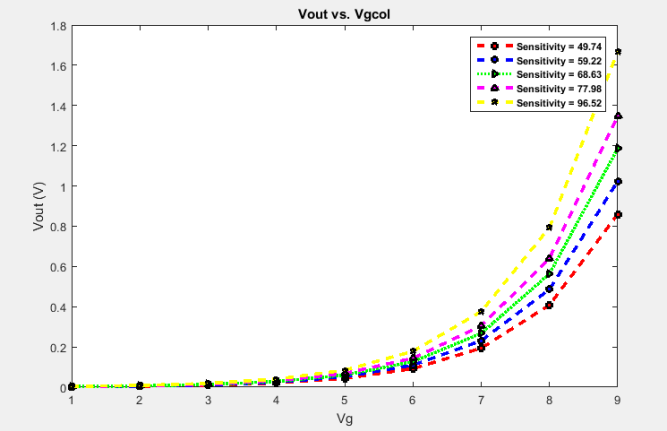

Figure 8. Sensitivity of sensor array model considering single column

Figure 8 presents the sensitivity of the sensor array model considering one of the columns of the 8 x 8 array model. The maximum voltage is approximately 1.7 V, and amplification of 8 is achieved with series connected biosensors. The sensitivity is improved by a factor of 4% as compared with the single biosensor model. Considering the outputs of eight columns processed together, the sensitivity of the 8 x 8 biosensor array model is increased by a factor of 32 as compared with the single sensor array model. The output of each column sensor array model is independently processed by the instrumentation amplifier (IA1 to IA8), and the eight outputs of the instrumentation amplifier are combined to generate the final output of the sensor array model. In this work, two methods are proposed to characterize the biosensor array outputs. Figure 9 presents the first method termed as "Digital Readout", and Figure 10 presents the second method, "Analog readout with reference". In the digital readout method, each of the eight outputs of the instrumentation amplifier is independently compared with reference voltages V1 to V8 in a comparator circuit to generate outputs T1 to T8, which are binary outputs. The thermometric decoder processes these eight outputs and converts it to 3-bit digital data indicating eight levels. Each of these eight levels classifies the biosensor array model into eight classes.

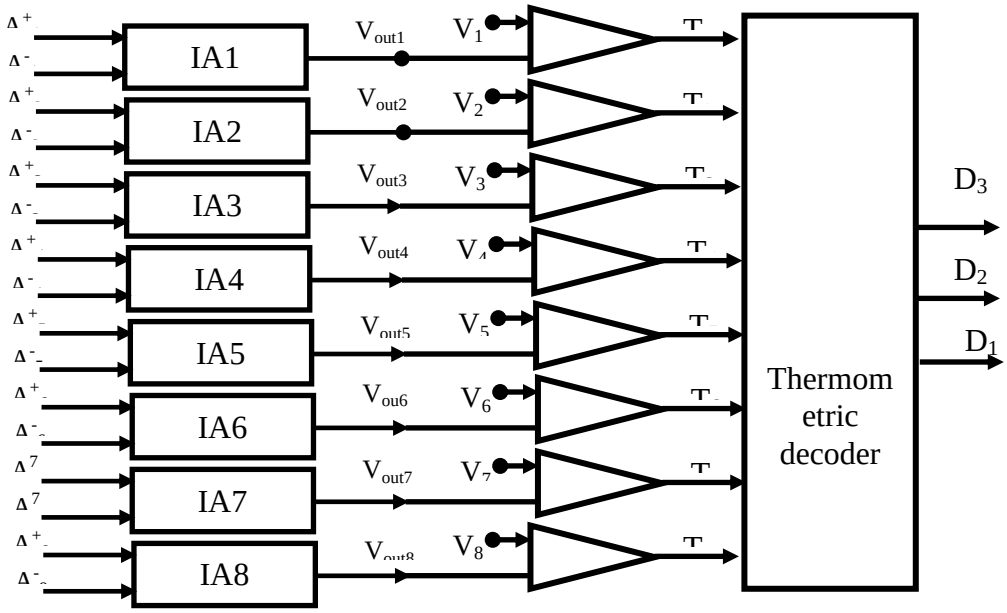

Figure 9. Digital readout models

Table 3*Digital readout circuit 1 outputs*

Gate voltage (Vg)	**Comparator output**	**Output**
	$T_8T_7T_6T_5$ $T_4T_3T_2T_1$	**D3 D2 D1**
0.11	0 0 0 0 0 0 0 1	000
0.12	0 0 0 0 0 0 1 1	001
0.13	0 0 0 0 0 1 1 1	010
0.14	0 0 0 0 1 1 1 1	011
0.15	0 0 0 1 1 1 1 1	100
0.16	0 0 1 1 1 1 1 1	101
0.17	0 1 1 1 1 1 1 1	110
0.18	1 1 1 1 1 1 1 1	111

In the analog readout model, two circuits are designed, as shown in Figure 10 and Figure 11. In the analog readout circuit 1, the outputs of each of the eight instrumentation amplifiers are given to an adder module, and the final output Vfinal is generated.

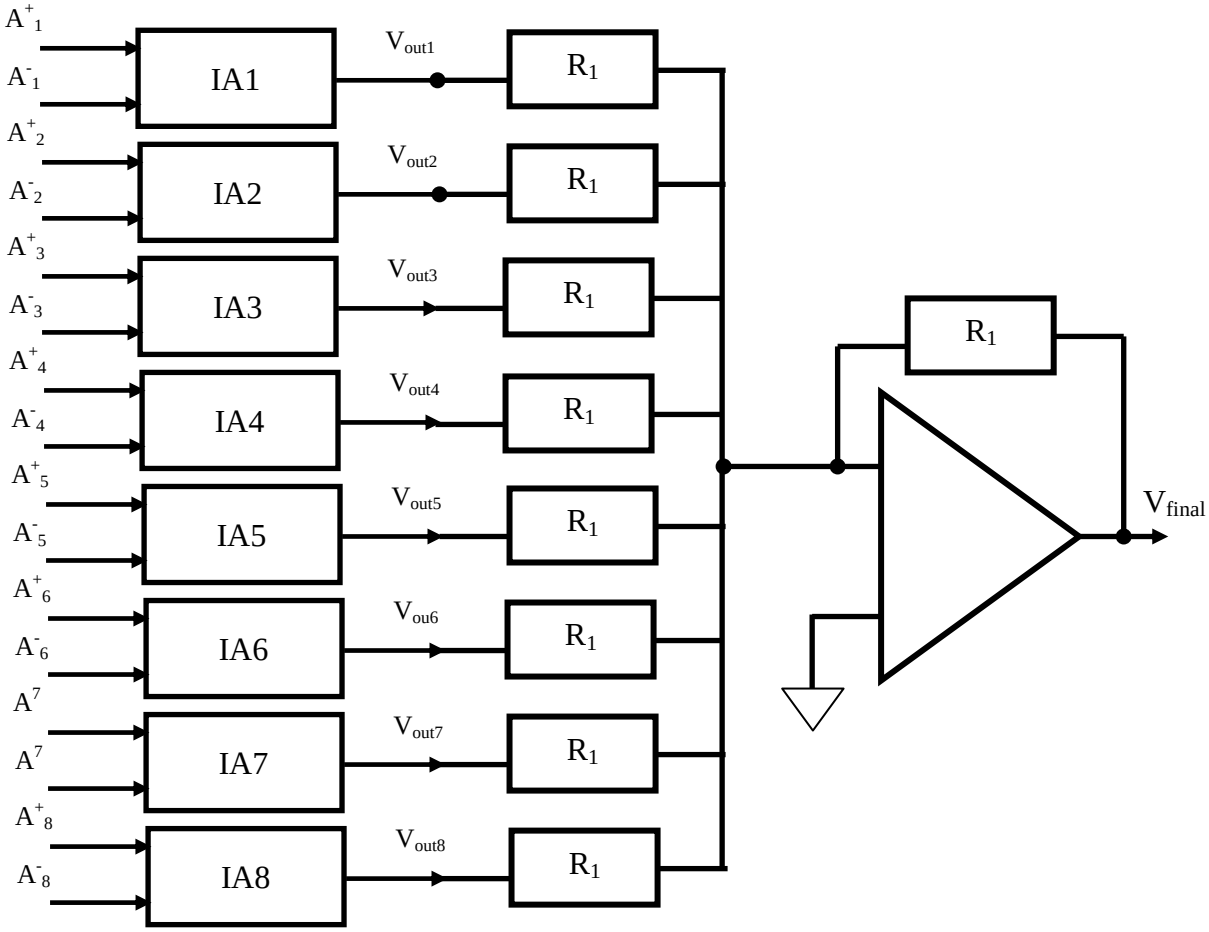

Figure 10. Analog readout circuit 1

Figure 11 presents the simulation results that compare the sensitivity of a single biosensor with array biosensor. The graph also presents the variation of Vout with regard to pH levels.

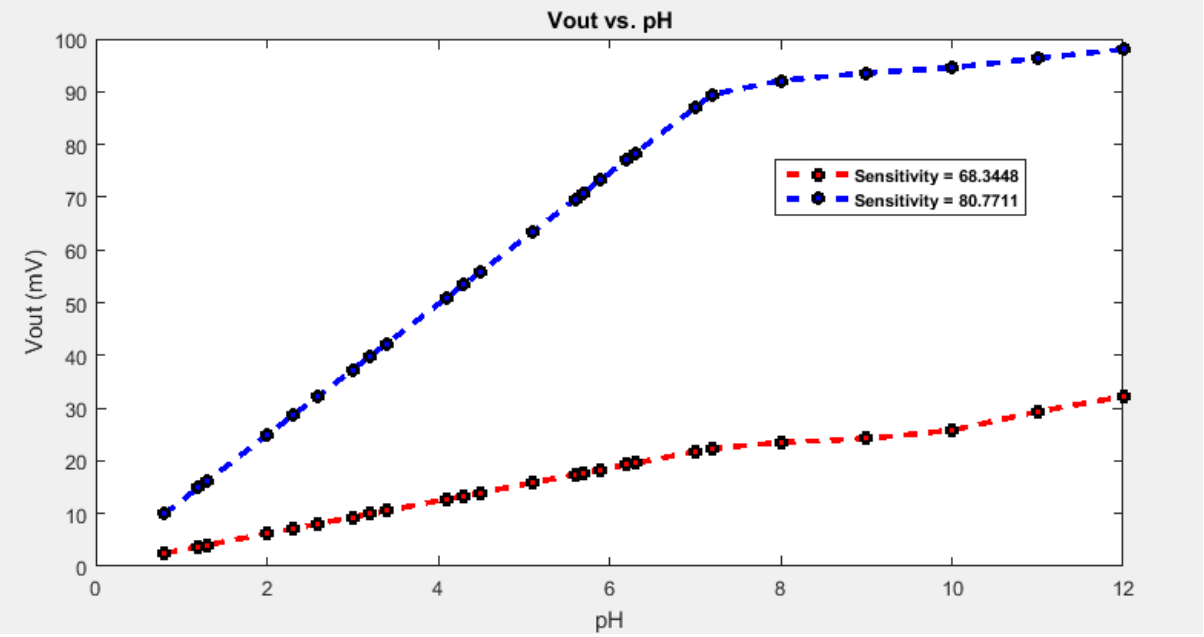

Figure 11. Comparing biosensor outputs with single sensor and array sensor models

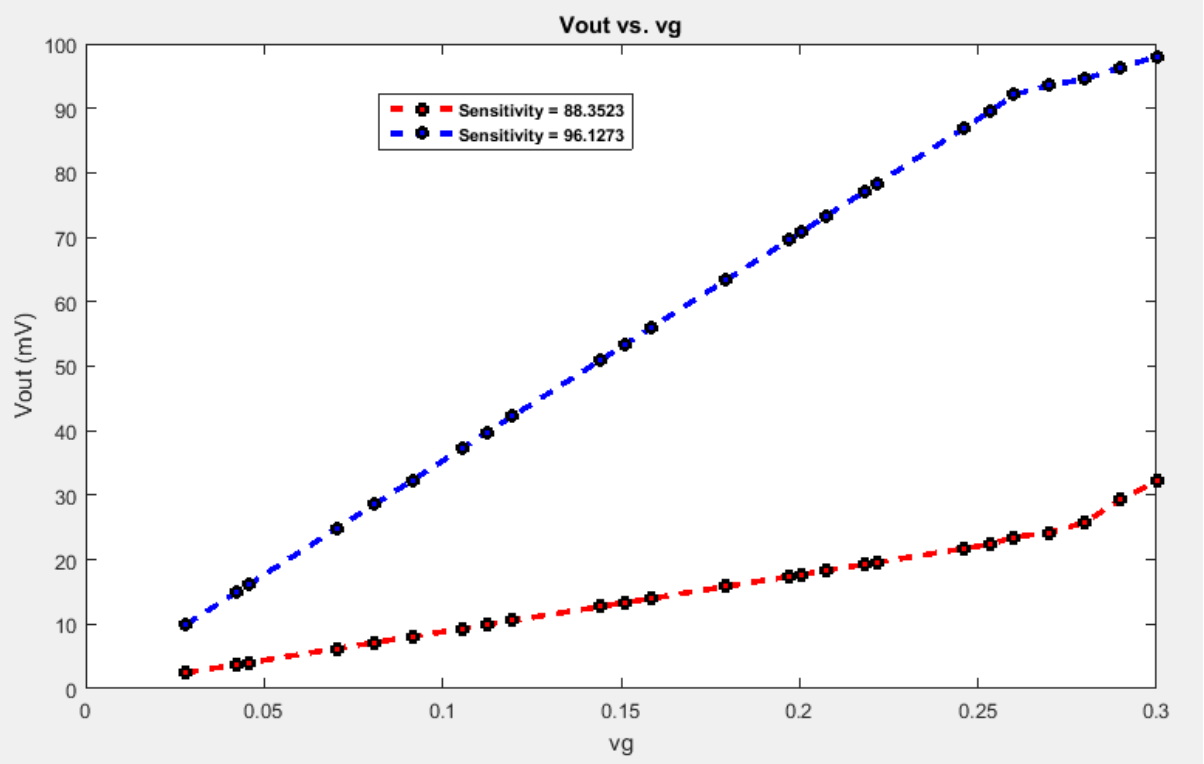

Figure 12. Comparison of output voltages with gate voltage

In Figure 12 comparison of the output voltage of the instrumentation amplifier with gate voltage is presented for both single sensor and array sensor models. The sensitivity of the array sensor model is higher than the single sensor model.

Figure 13 presents the analog readout model with reference. In this model, the first column and last column of the sensor array (i.e. column 1 and column 8) are biased with a reference voltage of 0.3 V.

The reference voltages of all other sensor array models (column 2 to column 7) are set with a reference bias voltage of 0.1 V. The analyte concentration and DNA biomarker-bioreceptor equivalent voltage represented by VBMEP are set to 0.1 V to 0.3 V. The output of first and last column is accumulated in the adder module (reference adder), and the outputs of all other column biosensors are accumulated in adder circuit. The outputs of both are compared and presented as in Figure 14.

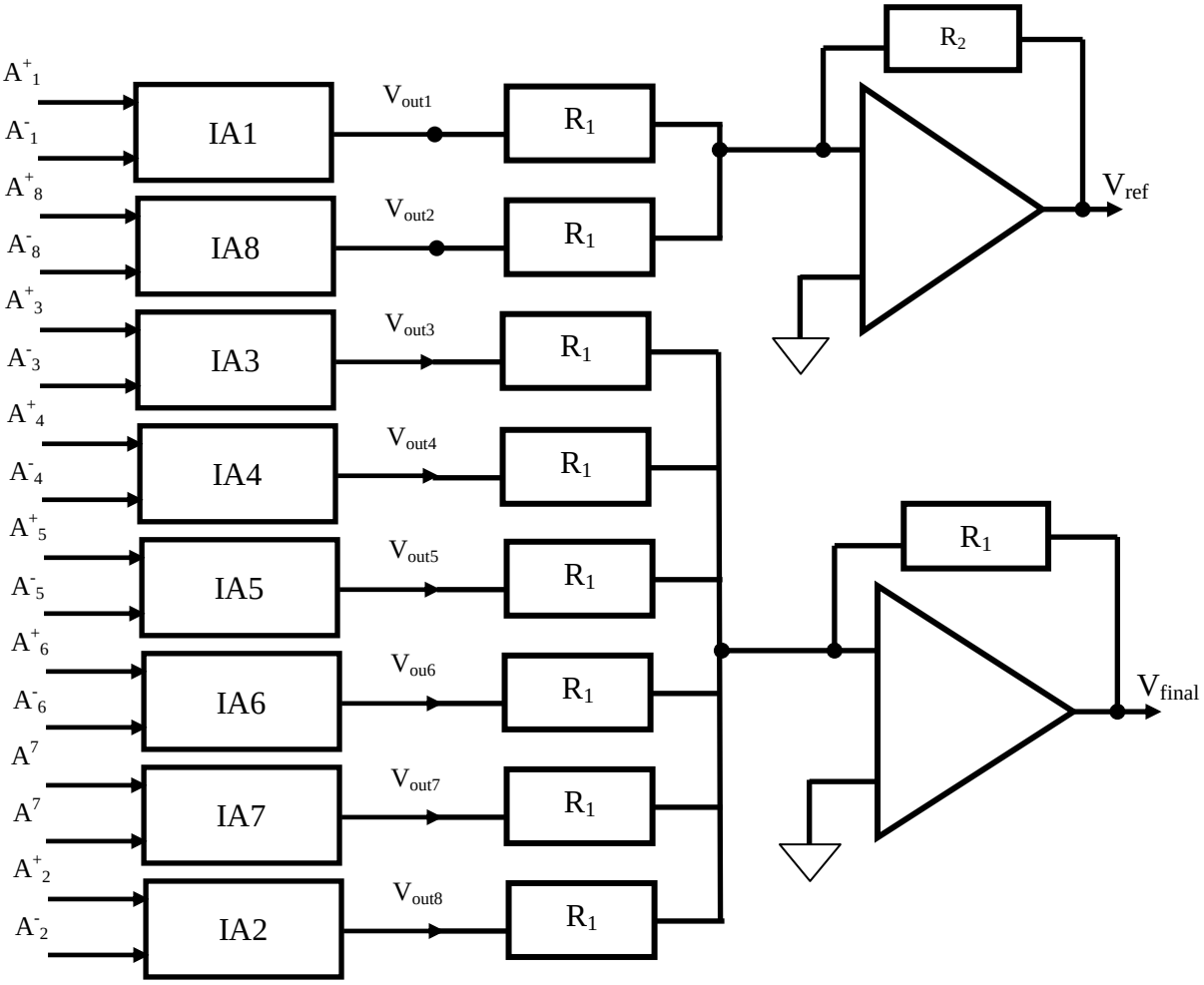

Figure 13. Analog readout model circuit 2

In circuit model 2, the gate voltage of the first column and last column are set to Vref alone, and the voltages of all other columns are Vg= Vref. + VBMEP. The output of IA1 and IA8 are accumulated in the adder 1 circuit to generate $V_{reffinal}$. The outputs of all other instrumentation amplifiers are accumulated in the second adder to generate Vfinal. Comparison of $V_{reffinal}$ with V_{final} is considered for characterization of biosensor array model.

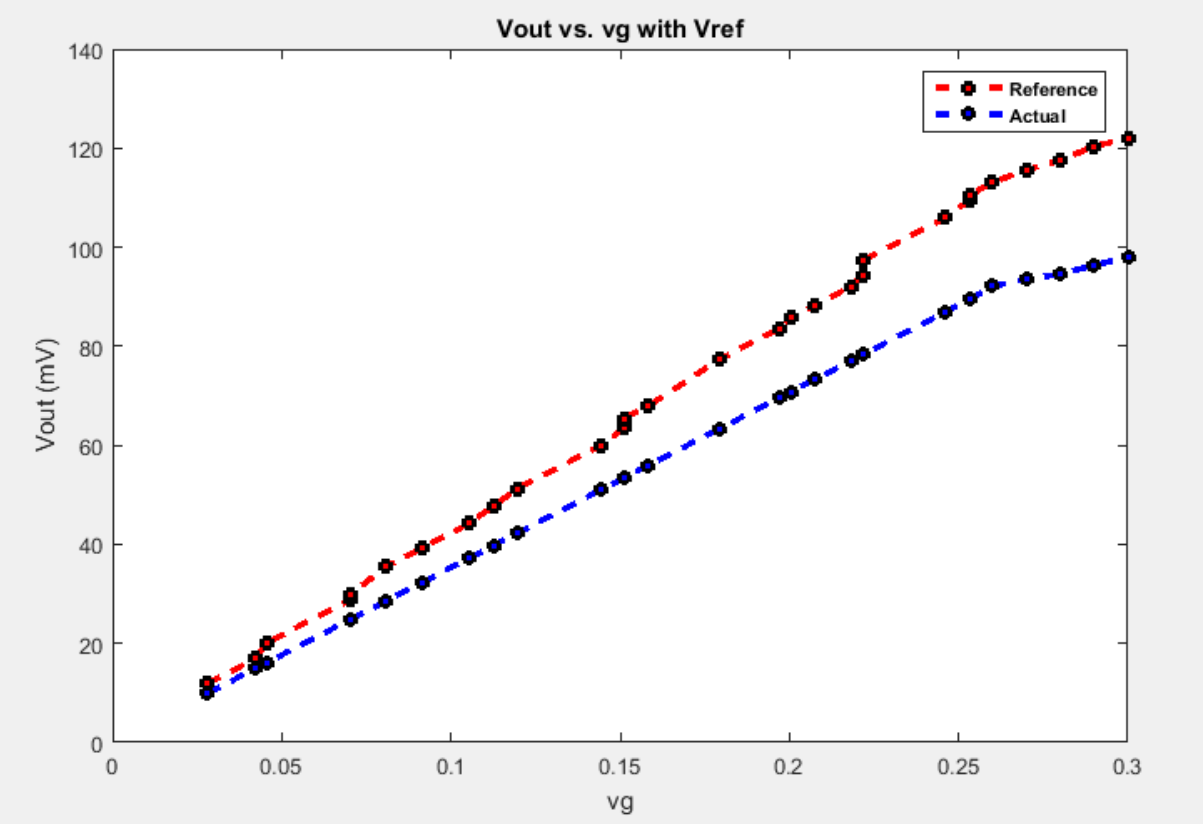

Figure 14. Output response of analog readout with reference

Conclusion

The design of biosensor array interfacing circuits is carried out using CNTFETs. The primary building blocks of interfacing circuit such as single stage amplifier, differential amplifier and operational amplifier are designed considering basic principles. The operational amplifier is designed to have a unity gain bandwidth of 1 GHz and a phase margin of 530. The wideband operational amplifier is stable and is designed with a trade-off for a high slew rate and stability. The biosensor is interfaced with instrumentation amplifier that comprises of three operational amplifiers. The front end of the instrumentation amplifier is made up of voltage followers, and the difference in voltage across the source and drain ends of the biosensor are considered for amplification. The second stage of the instrumentation amplifier has a high gain, and the voltage difference is amplified. The sensitivity is improved with a sensor array model that has eight columns of series connected biosensors. The 8 x 8 array model is interfaced with instrumentation amplifier, and the performances of the model are evaluated considering different biomarker electro potential equivalent voltages. The sensitivity of the series connected sensor array model is increased by a factor of 32 as compared with the single sensor array model. The 8 x 8 array model has a sensitivity of 96.12 compared with the single column sensor array model with a sensitivity of 88.3523. The analog readout circuit is designed with a reference electrode for real time comparison of the sensor array model.

References

1. Dalton, A.B.; Stephan, C.; Coleman, J.N.; McCarthy, B.; Ajayan, P.M.; Lefrant, S.; Bernier, P.; Blau, W.J.; Byrne, H.J. Selective interaction of a semiconjugated organic polymer with single-wall nanotubes. J. Phys. Chem. B 2000, 104, 10012–10016.

2. Dastagir, T.; Forzani, E.S.; Zhang, R.; Amlani, I.; Nagahara, L.A.; Tsui, R.; Tao, N. Electrical detection of hepatitis C virus RNA on single wall carbon nanotube-field effect transistors. Analyst 2007, 132, 738–740
3. Islam, M.F.; Rojas, E.; Bergey, D.M.; Johnson, A.T.; Yodh, A.G. High weight fraction surfactant solubilization of single-wall carbon nanotubes in water. Nano Lett. 2003, 3, 269–273
4. Kim, J.P.; Lee, B.Y.; Lee, J.; Hong, S.; Sim, S.J. Enhancement of sensitivity and specificity by surface modification of carbon nanotubes in diagnosis of prostate cancer based on carbon nanotube field effect transistors. Biosens. Bioelectron. 2009, 24, 3372–3378
5. Liu, H.; Chen, J.-G.; Wang, C.; Liu, Z.-T.; Li, Y.; Liu, Z.-W.; Xiao, J.; Lu, J. Immobilization of cyclometalated iridium complex onto multi walled carbon nanotubes for dehydrogenation of indolines in aqueous solution. Ind. Eng. Chem. Res. 2017, 56, 11413–11421
6. Ni, D.; Zhang, J.; Wang, X.; Qin, D.; Li, N.; Lu, W.; Chen, W. Hydroxyl radical-dominated catalytic oxidation in neutral condition by axially coordinated iron phthalocyanine on mercapto-functionalized carbon nanotubes. Indus. Eng. Chem. R. 2017, 56, 2899–2907Anılan, H., & Anagün, Ş.S. (2007). Öğretmen adaylarının kendi mesleki gelişimlerini değerlendirmeleri. *Proceedings of XVI. Ulusal Eğitim Bilimleri Kongresi,* 261-268.
7. Radha B. L, Cyril Prasanna Raj P, Dinesh Rangappa, Interface Circuit for array Biosensor, Indian Patent- CBR-27779, App. No. 202141034088, July 29, 2021(patent filed)
8. Rezaei, S.J.T.; Khorramabadi, H.; Hesami, A.; Ramazani, A.; Amani, R.; Ahmadi, R. Chemoselective reduction of nitro and nitrile compounds with magnetic carbon nanotubes-supported Pt(II) catalyst under mild conditions. Ind. Eng. Chem. Res. 2017, 56, 12256–12266
9. So, H.M.; Park, D.W.; Jeon, E.K.; Kim, Y.H.; Kim, B.S.; Lee, C.K.; Choi, S.Y.; Kim, S.C.; Chang, H.; Lee, J.O. Detection and titer estimation of Escherichia coli using aptamer-functionalized single-walled carbon-nanotube field-effect transistors. Small 2008, 4, 197–201
10. Stobinski, L.; Tomasik, P.; Lii, C.Y.; Chan, H.H.; Lin, H.M.; Liu, H.L.; Kao, C.T.; Lu, K.S. Single-walled carbon nanotube— Amylopectin complexes. Carbohyd. Polym. 2003, 51, 311–316
11. Thu, V.V.; Tam, P.D.; Dung, P.T. Rapid and label-free detection of H5N1 virus using carbon nanotube network field effect transistor. Curr. Appl. Phys. 2013, 13, 1311–1315
12. Villamizar, R.A.; Maroto, A.; Rius, F.X.; Inza, I.; Figueras, M.J. Fast detection of Salmonella Infantis with carbon nanotube field effect transistors. Biosens. Bioelectron. 2008, 24, 279–283